Journal of Chromatography A, 1218 (2011) 3823–3829

Contents lists available at ScienceDirect

Journal of Chromatography A

journal homepage: www.elsevier.com/locate/chroma

Separation of nanorods by density gradient centrifugation

Bin Xiong, Jing Cheng, Yanxia Qiao, Rui Zhou, Yan He*, Edward S. Yeung

College of Chemistry and Chemical Engineering, College of Biology, State Key Laboratory of Chemo/Biosensing and Chemometrics, Hunan University, Changsha 410082, China

ARTICLE INFO

Article history:
Received 26 December 2010
Received in revised form 11 April 2011
Accepted 12 April 2011
Available online 20 April 2011

Keywords:
Gold nanoparticle
Nanorods
Separation
Density gradient centrifugation

ABSTRACT

The experimental conditions necessary for the synthesis of well-defined nanoparticles are often difficult to control. There is thus a compelling need for post-synthesis separation of nanoparticles polydispersed in size and shape. We demonstrate here both theoretically and experimentally that gold nanorods with diverse aspect ratios can be separated using density gradient centrifugation. By analysing the force balance of a Brownian rod falling in a Stokes flow, we derive a rigorous and predictive model that reveals the quantitative dependency of the nanorod sedimentation rates on their mass and shape. The calculations show that while mass dependency is still the dominating factor during centrifugation, the shape factor is not insignificant. Relatively heavier but long and thin rods could sediment slower than certain size of lighter spheres, and some rods and spheres with different masses and shapes may never be separated. This mass and shape dependency is exploited to separate as-prepared gold nanorod colloids by sucrose gradient centrifugation. Two layers of nanorods with narrow aspect-ratio distributions are obtained.

1. Introduction

Nanometer-sized particles show unique physical and chemical properties that are different from those of bulk materials depending on their sizes and shapes due to the quantum confinement effect [1–5]. It is important to obtain monodispersed nanoparticles to define and exploit their distinct properties. Generally, two strategies have been employed to obtain products uniform in size and shape. One strategy is to optimize the nanocrystal growth parameters [6–9], but except for a few cases, most nanocrystal synthesis methods tend to result in polydispersed nanoparticles. The other approach is post-synthesis separation [10–14]. In recent years, a variety of methods, such as centrifugation [10,15–19], size exclusion chromatography [20,21], filtration or diafiltration [13,21], selective precipitation [22,23], selective oxidation or etching [24,25], and electrophoresis [11,14,20,26] have been utilized to produce certain nanoparticle fractions with narrow shape and size distributions. Among all methods for nanoparticle separation and purification, centrifugation is the most convenient as it does not rely on any liquid–solid phase interactions and specific chemical reactions. While differential centrifugation usually does not have precise control over the size, there have been many successes in separating nanoparticles with density gradient centrifugation for size, shape, and aggregation-state selection. For example, Sun [17] reported the separation of FeCo@C nanocomposites using iodixanol gradient solution and the separation of chemically modified graphene using sucrose gradient solution. Chen [15] isolated gold nanoparticle dimers and trimers by centrifugation with high density $CsCl_2$ solutions. Bai [18] exploited an effective method for rapid separation and purification of metal and CdSe nanoparticles by using a nonhydroxylic organic density gradient. These studies advanced the separation capability of density gradient centrifugation experimentally, but fell short in providing a predictive theoretical model to illustrate the separation process. Recently, Sharma [27] demonstrated that shape separation between gold nanospheres and nanorods could be readily achieved using centrifugation and offered a theoretical framework to explain this phenomenon. By providing expressions of the angular speed-normalized sedimentation rate and the sedimentation coefficient for both spherical and rod-shaped nanoparticles, they revealed that the shape–dependent drag causes particles to have shape–dependent sedimentation behaviour. However, their sedimentation coefficient expression for nanorods contains unknown orientational correction factors, which made it impossible to give quantitative predictions on the sedimentation rates of nanoparticles and nanorods of various sizes and aspect ratios.

Gold nanorods have been widely used in cancer cell diagnosis and photothermal therapy [28–30], drug and gene delivery and controlled release [31–33], and cellular imaging [34–36]. Uniform gold nanorods are especially needed for sensitive biosensing, accurately controlled release, two-photon and infrared imaging [37,38], and single nanorod orientation sensing [39,40]. Here, we modeled gold nanorods as Brownian ellipsoidal particles experiencing force balance in a Stokes flow in a pipe and derived a rigorous expression of the orientation averaged vertical sedimentation coefficient.

* Corresponding author. Tel.: +86 731 88823074; fax: +86 731 88821904.
E-mail address: yanhe2021@gmail.com (Y. He).

0021-9673/$ – see front matter © 2011 Elsevier B.V. All rights reserved.
doi:10.1016/j.chroma.2011.04.038

The validity of the expression is verified to be consistent with the classical sedimentation coefficient expression for spheres when the aspect ratio of rods is reduced to one. The sedimentation coefficient of a nanorod is both diameter/mass and aspect ratio dependent and increases monotonically with either parameter. So for Brownian rods during centrifugation in a viscous fluid, the sedimentation rate and the displacement can be calculated with known angular speed and centrifugal time. This allows us to investigate the centrifugal sedimentation behaviors of gold nanorods quantitatively. Our results show that while mass dependency is still the dominating factor, the shape factor is not insignificant. Relatively heavier but long and thin rods could sediment slower than certain size of lighter spheres, and some rods and spheres with different masses and shapes may never be separated with just centrifugation. Moreover, our sedimentation rate expression could be utilized to evaluate the separation efficiency of gold nanorods with density gradient centrifugation under various conditions. Appropriate composition and thickness of the gradient layers and the centrifugal time should be chosen for attaining the best isolation efficiency according to our calculation. Experimentally, centrifugal separation of as-prepared gold nanorods was achieved using a sucrose gradient solution. Two layers of gold nanorods with narrower aspect ratio distributions were obtained. The results are consistent with our theoretical analysis.

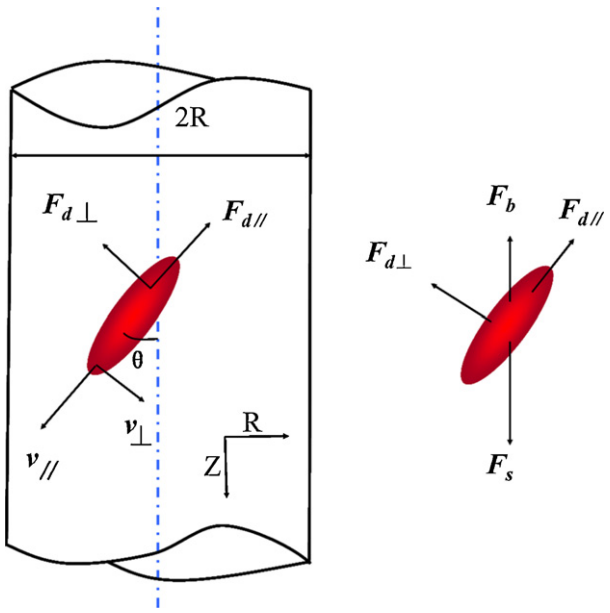

Fig. 1. Schematic illustration of the forces acting upon an ellipsoid during steady-state sedimentation.

2. Experimental

2.1. Preparation of density gradient sucrose solution

Sucrose solutions were prepared by dissolving pure sucrose (AMRESCO) in deionized water by heating while stirring. After cooling to room temperature, sucrose solutions with different mass fractions and a total volume of 1.5 mL were carefully added to the vials layer by layer. The gradient solution from top to bottom was made up of sucrose solutions with mass fractions of 20%, 30%, 40%, 50% and 60% with added volumes of 125 μL, 125 μL, 125 μL, 125 μL and 600 μL, respectively.

2.2. Synthesis and separation of gold nanorods

All the chemical reagents for gold nanorods synthesis were AR grade and purchased from Shanghai Sinopharm. Gold nanorods were synthesized using a seed mediated growth method and the procedure for gold nanorod preparation was described elsewhere [25,41]. For a typical density gradient separation, 150 μL crude gold nanorod colloid solution was added slowly onto the top of the gradient sucrose solution and centrifuged with an angular speed of 6000 rpm for 20 min (if not mentioned otherwise) by using an Eppendorf 5415D Centrifuge. After centrifugation, gold nanorods in each separated layer was taken out with a pipette and redispersed in deionized water.

3. Theory

For a particle under simple sedimentation diffusion equilibrium, we consider that the forces acting on a particle consist of centrifugal force, $F_c = m_p\omega^2 r$, buoyant force, $F_b = -m_p\omega^2 r(\rho_m/\rho_p)$, viscous drag force, $F_d = -\xi v$, and isotropic Brownian fluctuating force, F_f, where m_p is the mass of the particle, r is the distance from the center of the centrifuge to the location of the particle, ρ_p and ρ_m are the density of the particle and surrounding medium, ξ is the drag coefficient, and v is the velocity of particle sedimentation [27]. When these forces came to a balance, the sedimentation velocity normalized by the applied angular acceleration, which is called the sedimentation coefficient, S, can be obtained from the equation $m_p\omega^2 r - m_p\omega^2 r(\rho_m/\rho_p) - \xi v = 0$, that is, $S = v/\omega^2 r = m_p(1 - \rho_m/\rho_p)/\xi$. The drag coefficient ξ is related to the Reynolds number, Re, which is the ratio of the inertial forces to the viscous forces under given flow conditions. For nanometer-sized objects during sedimentation, $Re \ll 1$ and Stokes' law applies, so the expression of the drag coefficient for spherical nanoparticles is $\xi = 3\pi\eta d$, where η is the viscosity and d is the particle diameter. By substituting $m_p = 1/6\pi d^3\rho_p$, the sedimentation coefficient becomes $S = (\rho_p - \rho_m)d^2/18\eta$. For two gold or other nanoparticles with different masses, the sedimentation coefficients are different and therefore they can be separated using density gradient rate centrifugation as reported in the literature [15,17,18,42].

The rotation of non-spherical particles in the viscous flow has been thoroughly investigated in the past. Jeffery offered the exact rotation orbit of non-Brownian ellipsoidal particles in a viscous flow. Youngren and Acrivos [43] calculated the force and torque of cylindrical particles in simple shear flows. Intuitively, randomly oriented long cylindrical particles would be guided and eventually be aligned with the direction of flow or exhibit a biased orientational distribution [44]. However, in the case of rod-shape nanoparticles with $Re \ll 1$ in a simple Stokes flow, the rotational Brownian motion of the particles cannot be ignored. The orientational distribution function is affected by both the rotational diffusivities and the flow velocity, which act in competition with each other to respectively align and randomize the particle orientations [45]. A nanorod could make multiple rotations during the time it translates a distance comparable to its length, and the transient orientational distribution of the particles could be broad or even random. In that situation, the average sedimentation coefficient as well as the separation of rod-like nanoparticles would depend only on their drag coefficients, which should be simply a function of the shape of the particles.

Since the velocity of the flow is axially symmetrical, the motion of a nonspherical particle consists of a rotation in Z–R plane and a translation in the Z-axis direction (Fig. 1, an ellipsoidal rod is shown). We consider a prolate spheroid having length L along its axis of symmetry and diameter D at its equator, so its aspect ratio ϕ is given by L/D. The rigorous expressions of the drag force translating parallel and normal to the symmetrical axis of a prolate spheroid

have been determined for Stokes flow [46].

$$F_{\|} = \xi_{\|} v_{\|} = \frac{\phi^2 - 1}{(2\phi^2 - 1)/(\phi^2 - 1)^{1/2} \ln[\phi + (\phi^2 - 1)^{1/2}] - \phi} v_{\|} \quad (1)$$

$$F_{\perp} = \xi_{\perp} v_{\perp} = 8\pi\eta D \frac{\phi^2 - 1}{(2\phi^2 - 3)/(\phi^2 - 1)^{1/2} \ln[\phi + (\phi^2 - 1)^{1/2}] + \phi} v_{\perp} \quad (2)$$

Generally the drag coefficient of a particle in viscous flow was determined by the pressure of the particle experienced and is associated with the particular surface area. Since a rod and a prolate spheroid have almost the same surface area when their mass and aspect ratio are the same, we can use the above equation to describing the force acting on a nanorod during centrifugation. For a nanorod having an angle θ with the Z-axis, the two orthogonal drag forces can be transformed into another two orthogonal resistant forces comprising a vertical force, F_z, and a horizontal force, F_R. When this particle is in steady state sedimentation, force balance is required both in the vertical and horizontal directions, thus

$$F_Z = F_{||} \cos\theta + F_{\perp} \sin\theta - m_p \left(1 - \frac{\rho_m}{\rho_p}\right) \omega^2 r = 0 \quad (3)$$

$$F_R = F_{||} \sin\theta - F_{\perp} \cos\theta = 0 \quad (4)$$

The resistant forces in the vertical and horizontal direction can be solved with $\sin^2\theta + \cos^2\theta = 1$. So the corresponding instantaneous velocities in the two directions, v_Z and v_R, can be obtained from the following equations,

$$v_Z = v_{||} \cos\theta + v_{\perp} \sin\theta = \left(\frac{1}{\xi_{||}} \cos^2\theta + \frac{1}{\xi_{\perp}} \sin^2\theta\right) m_p \left(1 - \frac{\rho_m}{\rho_p}\right) \omega^2 r \quad (5)$$

$$v_R = v_{||} \cos\theta + v_{\perp} \sin\theta = \left(\frac{1}{\xi_{||}} - \frac{1}{\xi_{\perp}}\right) m_p \left(1 - \frac{\rho_m}{\rho_p}\right) \omega^2 r \sin\theta \cos\theta \quad (6)$$

The vertical velocity v_Z determines the sedimentation displacement and dictates whether separation of particles of different aspect ratios can be achieved. Generally, rods and other rotational symmetrical bodies are neutrally stable in any orientation without external orienting forces and $Re \leq 0.05$ [47]. For Brownian nanospheres and nanorods with diameters of several tens of nanometers under steady state sedimentation, Reynolds numbers have a magnitude of about 10^{-4}, and when force balance is considered, the orientation of rotational angle θ should be random. Since the θ value of ensemble nanorods is randomized due to their rotational Brownian motion, we can obtain the orientation-averaged vertical velocity by the following integral,

$$\bar{v}_z = \frac{1}{2\pi} \int_0^{2\pi} v_z d\theta = \frac{1}{2\pi} m_p \left(1 - \frac{\rho_m}{\rho_p}\right) \omega^2 r \int_0^{2\pi} \times \left(\frac{1}{\xi_{||}} \cos^2\theta + \frac{1}{\xi_{\perp}} \sin^2\theta\right) d\theta = m_p \left(1 - \frac{\rho_m}{\rho_p}\right) \omega^2 r \frac{\xi_{||} + \xi_{\perp}}{2\xi_{||}\xi_{\perp}} \quad (7)$$

To prove if such an integral is valid experimentally for the gold nanorod solutions being studied, we performed centrifugation of a commercial gold nanorod sample (average $L = 74$ nm and $D = 25$ nm from NanoPartz, still polydispersed according to the TEM results, data not shown) in a highly viscous sucrose solution (60 wt%, $\eta = 58.93$ cp at 20 °C) at 3000, 6000 and 12,000 rpm for 80, 20 and 5 min, respectively. After centrifugation, the sedimentation displacement of each nanorod band was about the same i.e. 5.3 mm, 5.3 mm and 5.4 mm, respectively, indicating that their angular acceleration normalized vertical velocity was constant. We then calculated the time of a gold nanorod needed to make a full rotation and to translate a distance of its own length. The time τ_{rot} required for a rotational revolution is 5.7 ms according to equation [48]

$$\tau_{rot} = \frac{\pi\eta L^3}{3k_B T \ln(L/D)} \quad (8)$$

where k_B is the Boltzmann constant and T is the absolute temperature. However, the time of a nanorod ($L = 74$ nm and $D = 25$ nm) to travel a distance equal to its length in the highly viscous sucrose is 67.0 ms, 16.8 ms and 4.1 ms at 3000, 6000 and 12,000 rpm, respectively. It can be seen clearly that these sedimentation times are comparable to multiples of τ_{rot}, so the Brownian rotation of gold nanorods should play a significant role here. The above results suggest that the orientation distribution of the gold nanorods is randomized and the average vertical velocity obtained is valid.

From the definition of the sedimentation coefficient and by substituting $m_p = 1/6\pi D^3 \phi\ \rho_p$ into Eq. (7), we obtain the orientation-averaged sedimentation coefficient in the vertical direction,

$$\bar{S}_Z = \bar{v}_Z/\omega^2 r = m_p \left(1 - \frac{\rho_m}{\rho_p}\right) \frac{\xi_{||} + \xi_{\perp}}{2\xi_{||}\xi_{\perp}} = \frac{\pi D^2 \phi}{12\eta} (\rho_p - \rho_m) \frac{\Omega_{||} + \Omega_{\perp}}{\Omega_{||}\Omega_{\perp}} \quad (9)$$

By aid of the substitutions

$$\Omega_{||} = \frac{\xi_{||}}{\eta D} = 4\pi \frac{\phi^2 - 1}{(2\phi^2 - 1)/(\phi^2 - 1)^{1/2} \ln[\phi + (\phi^2 - 1)^{1/2}] - \phi}$$

$$\Omega_{\perp} = \frac{\xi_{\perp}}{\eta D} = 8\pi \frac{\phi^2 - 1}{2\phi^2 - 3/(\phi^2 - 1)^{1/2} \ln[\phi + (\phi^2 - 1)^{1/2}] + \phi}.$$

We noticed that the above expression for rods can be reduced to the classical expression of the sedimentation coefficient for spherical particles when the aspect ratio is very close to one. This is a direct evidence of the validity of our deduction. However, we failed to obtain the same result using the expression provided by Sharma [27] due to the unknown correction factors, so our theory is more robust. Some earlier studies also considered the hydrodynamic interaction between particles and surrounding fluid. But that effect is closely related to the concentration of particles. Since the concentration of nanorod colloids is usually very low, this effect was quite weak and can be ignored in our derivation.

4. Results and discussion

Because all the parameters in the above expression can be obtained experimentally, we can establish a predictive model to evaluate the sedimentation behaviors of nanorods of various diameters and aspect ratios during centrifugation in different viscous fluids. Fig. 2A shows the calculated sedimentation coefficients of rod-like particles with the same volume (mass) as a nanorod of $L = 74$ nm and $D = 25$ nm but with different aspect ratios during centrifugation in the sucrose solution. It can be seen that when having the same mass, longer and thinner rods always sediment more slowly than shorter and fatter ones, while spherical particles have the largest velocity. With the increase of sucrose mass fraction or the viscosity of the fluid, the sedimentation coefficients as well as the difference between nanorods with different aspect ratios decrease. Fig. 2B shows the relationship between the vertical sedimentation coefficients of nanorods and their diameters

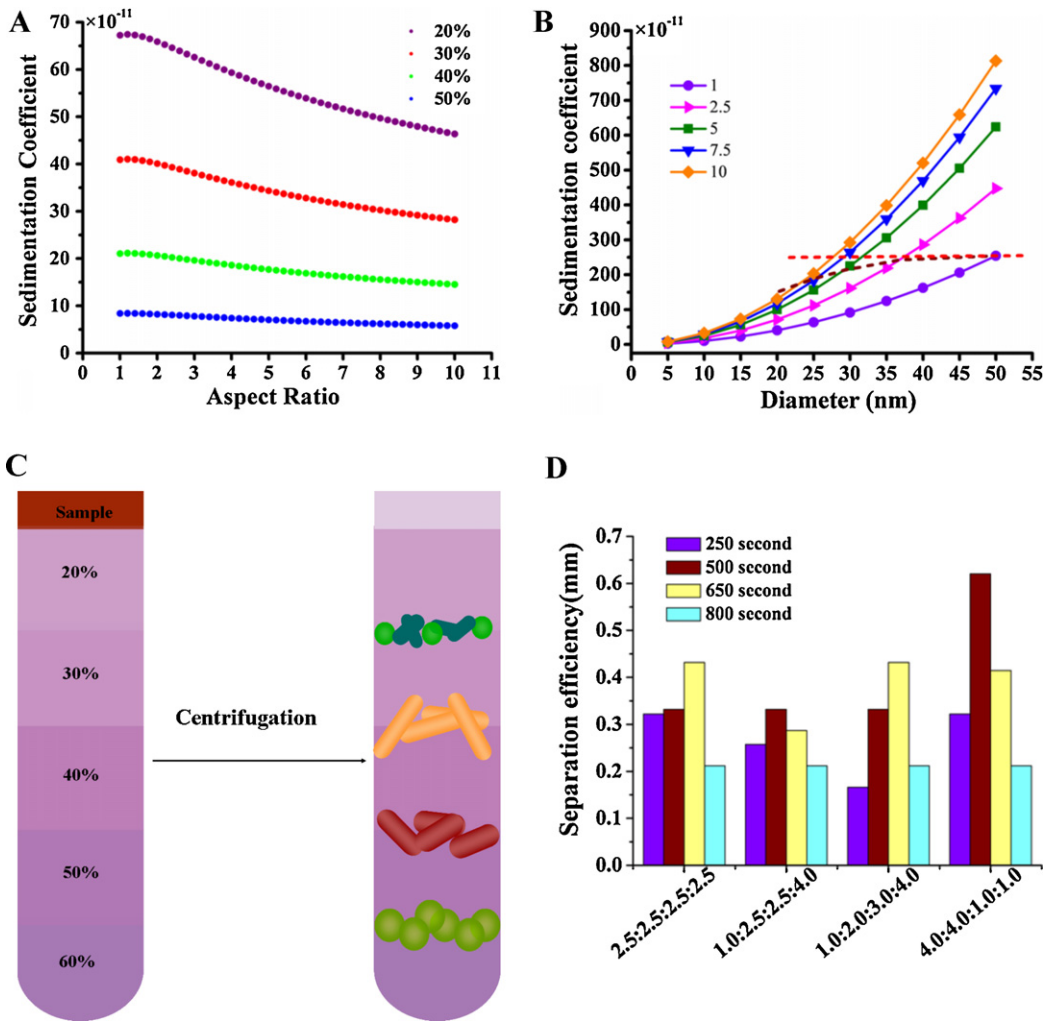

Fig. 2. (A) Orientation-averaged sedimentation coefficients in the vertical direction for nanorods with various aspect ratio but the same mass under sedimentation equilibrium in sucrose solution with different mass fraction. (B) Sedimentation coefficient as a function of the diameter and aspect ratio of the nanorods. The dashed curves linked particles with the same mass and the dashed horizontal line marked particles with the same sedimentation rate. (C) Predicated separation profile of a complicated sample containing rods with diverse aspect ratios and spheres with different diameters. (D) Calculated separation efficiency of two equal-mass gold nanorods of aspect ratios 2 and 4, respectively, during sucrose gradient centrifugation using different sucrose layer thickness and centrifugal time. The compositions of the 4 sucrose layers were all 20%, 30%, 40% and 50%.

and aspect ratios. It can be seen that the sedimentation coefficient increases with the diameter for rods with the same aspect ratio, and it also increases with the aspect ratio for rods with the same diameter. This is consistent with the usual knowledge that heavier particles sediment faster because the mass of the rods increase monotonically with either the diameter or the aspect ratio. However, not all particles with larger mass would fall faster than lighter ones. Also shown in Fig. 2B are one dashed curve linking rods with the same mass (essentially the same information as Fig. 2A) and one horizontal line marking particles with the same sedimentation coefficients. Because the equal-mass curve bends downward for rods with smaller diameters and higher aspect ratios, the particles in the triangular region that is above the dashed curve but below the dashed line will all have larger masses but slower sedimenta-

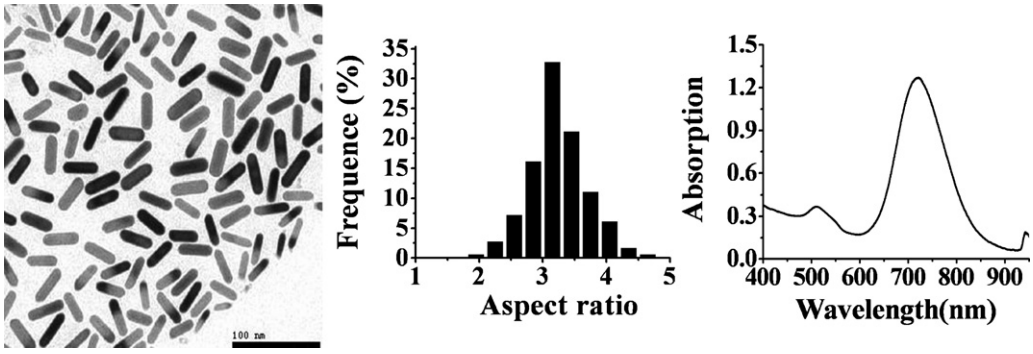

Fig. 3. TEM image, distribution of the average aspect ratio and UV–visible spectrum of the mother solution of the as-prepared gold nanorods.

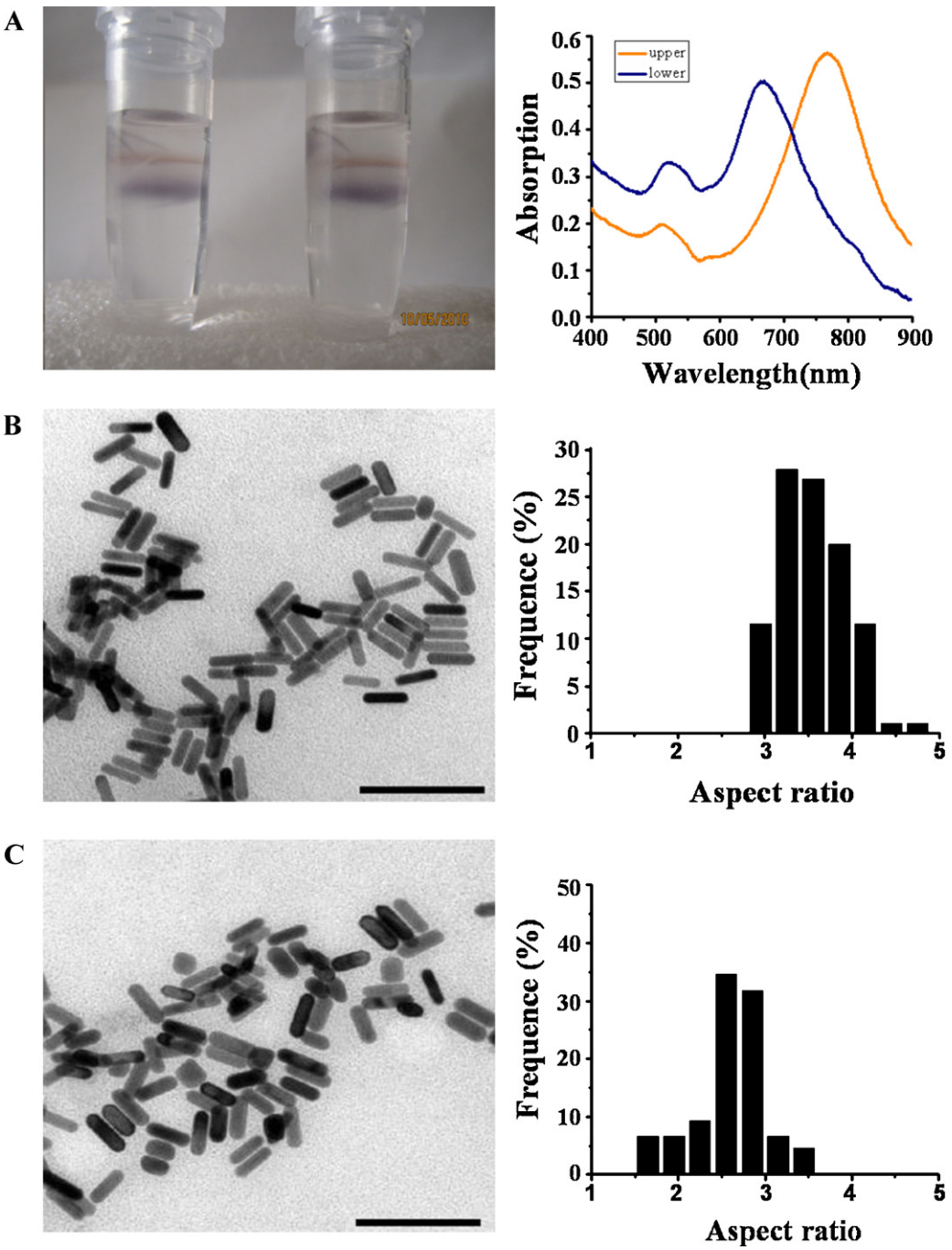

Fig. 4. Density gradient separation of the as-prepared gold nanorods. (A) Optical image of the centrifuge tube and the UV–visible spectra of the two layers after separation. (B) TEM image and aspect ratio distribution of nanorods from (B) the upper layer, and (C) the lower layer. All particles and rods with aspect ratio less than 1.5 were not counted and did not show up in the histogram data. The scale bar is 100 nm.

tion rates than the spherical particle at the cross point of the curve and the line. Moreover, for particles on the horizontal line that have the same sedimentation rate, the ones to the left are always heavier than the ones to the right, indicating that this set of particles with various diameters, aspect ratios and masses will never be separated by centrifugation. In other words, while centrifugation can be used for nanorods separation and purification, truly uniform nanorods cannot be obtained by this method alone. In contrast, theoretically nanospheres uniform in size could be separated from other spherical particles with just centrifugation. Based on the above analysis, we can obtain a general understanding of centrifugal separation of a heterogeneous nanorod colloid mixture, i.e. larger spheres have the fastest sedimentation rate, followed by short and fat rods and then long and thin rods with similar mass as the sphere, lighter spheres and rods would sediment last (Fig. 2C).

For particles with dimension distributions that can be separated by centrifugation, step-layer gradients are often used to improve the separation efficiency [17]. Increased resistance due to increasing density and viscosity will make particles with similar sedimentation rate to stop at certain locations and form a layer at an appropriate time window. But the separation efficiency could vary with the composition and thickness of each gradient layer and the centrifugal time. Fig. 2D shows the calculated separation distance of two gold nanorods with aspect ratios 2 and 4, respectively, but

with the same mass under various conditions using sucrose gradient centrifugation. We assume that sedimentation equilibrium can be achieved quickly and the slowing down of the rods at the layer boundaries is ignored. It can be seen that the separation distance is dependent on both the centrifugal time and the volume ratio of each layer in gradients. Notice that longer centrifugal time does not necessarily result in better separation efficiency. Therefore an optimized set of parameters should be chosen for each nanoparticle sample, and our predictive sedimentation rate equation could be used to evaluate the performance of density gradient centrifugation under various conditions.

According to our theoretical analysis, nanoparticles with different diameters or aspect ratios could have different sedimentation rates. This property can be exploited to separate or purify nanoparticle solutions using density gradient centrifugation. As a demonstration, we synthesized gold nanorods using a seed mediated growth method. Fig. 3 shows the TEM image, the extinction spectrum, and the aspect ratio histogram of the as-prepared gold nanorod colloids. The TEM image indicates that the mother solution contains a mixture of gold nanorods and a very small fraction of gold nanospheres. The spheres have an average diameter of 24 nm, whereas the rods have an average a diameter of 11.5 ± 1.8 nm, a length of 36.9 ± 5.4 nm, and an aspect ratio of 3.2 ± 0.4. After counting a total of 800 particles, the percentage of spheres was found to be less than 9%. The UV–visible spectrum also shows that rods are dominant in the mother solution as the intensity of the longitudinal surface plasmon peak at 720 nm is much higher than the intensity of transverse surface plasmon peak at 510 nm. The aspect-ratio histogram is constructed by analysing 500 rods from TEM images. The wide distribution of aspect ratios indicates that the rods are not uniform in shape.

We used step-layer gradient sucrose solutions (20%, 30%, 40%, 50% and 60%) as the separation medium. Fig. 4 shows the optical image, UV–visible spectra, and the TEM images and analysis results after a typical sucrose gradient centrifugation of the as-prepared gold nanorod solution. Two well-separated layers of particles could be clearly observed and the extinction peaks were at 767 nm and 670 nm, respectively. Compared to the extinction spectrum of the mother solution, the upper layer show a red shift and the lower layer show a blue shift, indicating that the aspect ratio distributions of the nanorods changed in both layers. The TEM images reveal that the upper layer mostly contained relatively long and thin rods plus a few small spheres (<3%), and the lower layer was mainly composed of relatively short and fat rods plus a few large spheres. This is consistent with our theoretical analysis that certain range of rods can never be separated from certain size of spheres. For each layer, 300 rods were analysed to obtain their size and aspect ratio distribution. The average length, diameter and the aspect ratio of rods in the upper layer are 36.5 ± 3.4 nm, 10.4 ± 1.2 nm and 3.5 ± 0.3, respectively. The average length, diameter and the aspect ratio of rods in the lower layer are 34.7 ± 5.7 nm, 13.4 ± 1.9 nm and 2.6 ± 0.4, respectively. Compared with the mother solution, the particles from either layer show an obvious improvement in both shape and size uniformity. Moreover, either collected fraction show little sign of aggregation and can be further purified for typical sensing experiments of gold nanorods. Based on their dimensions, the rods in the lower layer are 1.5 times as heavy as the rods in the upper layer, but the aspect ratio of the latter is 1.3 times of the former. The calculated sedimentation coefficient difference between the two rods is about 8% larger than that between two spheres with comparable masses. So their separation is still mainly due to the difference in mass, but the shape-related drag coefficient also plays a significant role. Generally, heavier nanoparticles would sediment faster than lighter particles based on the so-called mass dependent separation. Once the shape effect is considered, however, the sedimentation coefficient of nonspherical particles would be both shape and mass dependent. Therefore, larger nonspherical particles such as rods and plates might not always fall faster than smaller spheres during practical sedimentation. This is why the shape separation efficiency is always less than one. For separation of particles with the same shape such as rod–rod and plate–plate separation, density gradient centrifugation is still effective when these particles have similar masses.

5. Conclusions

We successfully applied density gradient centrifugation method to achieve aspect ratio separation of gold nanorods. By analysing the force balance upon a nanorod in a Stokes flow in a pipe, we obtained a rigorous expression that can quantitatively elucidate the sedimentation behaviour of nanorods. During steady state sedimentation, nanorods undergo rotational Brownian motion, resulting in the characteristic orientation-averaged sedimentation coefficient that is a function of the mass, diameter and aspect ratio of the rods. Thus nanorods with the same mass but diverse aspect ratios can be separated. Our theoretical analysis is consistent with experimental separation/purification of as-prepared gold nanorod solution using sucrose gradient centrifugation. Two layers of nanorods with distinct and sharp aspect ratio distributions were obtained. Our theoretical framework could be further exploited for evaluating separation and purification of other types of nonspherical nanoparticles.

Acknowledgement

This work was supported by NSFC 20975036, Program for New Century Excellent Talents in University and Hunan University 985 fund. E.S.Y. thanks the Ames Laboratory for partial support of this work.

Appendix A. Appendix

Deduction of the expression of the sedimentation coefficient of a prolate spheroid or rod in simple sedimentation diffusion equilibrium was based on the requirement that the forces acting on the particles come to a balance.

$$F_Z = F_{||} \cos\theta + F_{\perp} \sin\theta - m_p \left(1 - \frac{\rho_m}{\rho_p}\right) \omega^2 r = 0 \tag{1a}$$

$$F_R = F_{||} \sin\theta - F_{\perp} \cos\theta = 0 \tag{2a}$$

By substituting $F = \xi v$ we can get

$$\xi_{||} v_{||} \cos\theta + \xi_{\perp} v_{\perp} \sin\theta = m_p \left(1 - \frac{\rho_m}{\rho_p}\right) \omega^2 r \tag{3a}$$

$$\xi_{||} v_{||} \sin\theta = \xi_{\perp} v_{\perp} \cos\theta \tag{4a}$$

Multiply Eq. (3a) with $\cos\theta$ and substitute Eq. (4a),

$$\xi_{||} v_{||} \cos^2\theta + \xi_{\perp} v_{\perp} \cos\theta \sin\theta = m_p \left(1 - \frac{\rho_m}{\rho_p}\right) \omega^2 r \cos\theta \tag{5a}$$

$$\xi_{||} v_{||} \cos^2\theta + \xi_{||} v_{||} \sin^2\theta = m_p \left(1 - \frac{\rho_m}{\rho_p}\right) \omega^2 r \cos\theta \tag{6a}$$

Since $\sin^2\theta + \cos^2\theta = 1$, we can get the expression of $v_{||}$ and $v_{\perp}$.

$$v_{||} = m_p \left(1 - \frac{\rho_m}{\rho_p}\right) \frac{\omega^2 r \cos\theta}{\xi_{||}} \tag{7a}$$

$$v_{\perp} = m_p \left(1 - \frac{\rho_m}{\rho_p}\right) \frac{\omega^2 r \sin\theta}{\xi_{\perp}} \tag{8a}$$

So the corresponding instantaneous velocities in the two directions, v_Z and v_R, are given by

$$v_Z = v_{||}\cos\theta + v_{\perp}\sin\theta = \left(\frac{1}{\xi_{||}}\cos^2\theta + \frac{1}{\xi_{\perp}}\sin^2\theta\right) m_p\left(1-\frac{\rho_m}{\rho_p}\right)\omega^2 r \tag{9a}$$

$$v_R = v_{||}\cos\theta + v_{\perp}\sin\theta = \left(\frac{1}{\xi_{||}} - \frac{1}{\xi_{\perp}}\right) m_p\left(1-\frac{\rho_m}{\rho_p}\right)\omega^2 r\sin\theta\cos\theta \tag{10a}$$

The average vertical velocity of a Brownian prolate spheroid in sedimentation was obtained by the integral

$$\begin{aligned}\bar{v}_z &= \frac{1}{2\pi}\int_0^{2\pi} v_z d\theta = \frac{1}{2\pi} m_p\left(1-\frac{\rho_m}{\rho_p}\right)\omega^2 r\int_0^{2\pi}\left(\frac{1}{\xi_{||}}\cos^2\theta + \frac{1}{\xi_{\perp}}\sin^2\theta\right)d\theta \\ &= \frac{1}{2\pi} m_p\left(1-\frac{\rho_m}{\rho_p}\right)\omega^2 r\int_0^{2\pi}\left(\frac{1}{2\xi_{||}}(\cos 2\theta+1) + \frac{1}{2\xi_{\perp}}(1-\cos 2\theta)\right)d\theta \\ &= \frac{1}{2\pi} m_p\left(1-\frac{\rho_m}{\rho_p}\right)\omega^2 r\int_0^{2\pi}\left(\frac{1}{2\xi_{||}} + \frac{1}{2\xi_{\perp}}\right)d\theta + \frac{1}{2\pi} m_p\left(1-\frac{\rho_m}{\rho_p}\right)\omega^2 r \\ &\quad \int_0^{2\pi}\left(\frac{1}{2\xi}\cos 2\theta - \frac{1}{2\xi_{\perp}}\cos 2\theta\right)d\theta = m_p\left(1-\frac{\rho_m}{\rho_p}\right)\omega^2 r\frac{\xi_{||}+\xi_{\perp}}{2\xi_{||}\xi_{\perp}}\end{aligned} \tag{11a}$$

From the definition of the sedimentation coefficient and by substituting the mass expression of a prolate spheroid $m_p = 1/6\pi D^3\phi\,\rho_p$ into Eq. (11a), the orientation-averaged sedimentation coefficient in the vertical direction is given by the follows equation

$$\bar{S}_Z = \frac{\bar{v}_Z}{\omega^2 r} = m_p\left(1-\frac{\rho_m}{\rho_p}\right)\frac{\xi_{||}+\xi_{\perp}}{2\xi_{||}\xi_{\perp}} = \frac{\pi D^2\phi}{12\eta}(\rho_p-\rho_m)\frac{\Omega_{||}+\Omega_{\perp}}{\Omega_{||}\Omega_{\perp}} \tag{12a}$$

By applying the substitutions

$$\Omega_{||} = \frac{\xi_{||}}{\eta D} = 4\pi\frac{\phi^2-1}{(2\phi^2-1)/(\phi^2-1)^{1/2}\ln[\phi+(\phi^2-1)^{1/2}]+\phi}$$

$$\Omega_{\perp} = \frac{\xi_{\perp}}{\eta D} = 4\pi\frac{\phi^2-1}{(2\phi^2-3)/(\phi^2-1)^{1/2}\ln[\phi+(\phi^2-1)^{1/2}]-\phi}$$

References

[1] A. Henglein, J. Phys. Chem. 97 (1993) 5457.
[2] C.P. Collier, R.J. Saykally, J.J. Shiang, S.E. Henrichs, J.R. Heath, Science 277 (1997) 1978.
[3] S.H. Kim, G. Medeiros-Ribeiro, D.A.A. Ohlberg, R.S. Williams, J.R. Heath, J. Phys. Chem. B 103 (1999) 10341.
[4] K.C. Beverly, J.F. Sampaio, J.R. Heath, J. Phys. Chem. B 106 (2002) 2131.
[5] C. Burda, X. Chen, R. Narayanan, M.A. El-Sayed, Chem. Rev. 105 (2005) 1025.
[6] Y.G. Sun, Y.N. Xia, Science 298 (2002) 2176.
[7] T.K. Sau, C.J. Murphy, J. Am. Chem. Soc. 126 (2004) 8648.
[8] X. Wang, Y.D. Li, Chem. Commun. (2007) 2901.
[9] S.D.C. Perrault, J. Am. Chem. Soc. 131 (2009) 17042.
[10] M.S. Arnold, S.I. Stupp, M.C. Hersam, Nano Lett. 5 (2005) 713.
[11] J.P.A. Isabelle Arnaud, C. Roussel, H.H. Girault, Chem. Commun. (2005) 787.
[12] K.M. Krueger, A.M. Al-Somali, J.C. Falkner, V.L. Colvin, Anal. Chem. 77 (2005) 3511.
[13] S.F. Sweeney, G.H. Woehrle, J.E. Hutchison, J. Am. Chem. Soc. 128 (2006) 3190.
[14] M. Hanauer, S. Pierrat, I. Zins, A. Lotz, C. Sonnichsen, Nano Lett. 7 (2007) 2881.
[15] G. Chen, Y. Wang, L.H. Tan, M.X. Yang, L.S. Tan, Y. Chen, H.Y. Chen, J. Am. Chem. Soc. 131 (2009) 4218.
[16] J.A. Jamison, K.M. Krueger, J.T. Mayo, C.T. Yavuz, J.J. Redden, V.L. Colvin, Nanotechnology 20 (2009) 355702.
[17] X.M. Sun, S.M. Tabakman, W.S. Seo, L. Zhang, G.Y. Zhang, S. Sherlock, L. Bai, H.J. Dai, Angew. Chem. Int. Ed. 48 (2009) 939.
[18] L. Bai, X.J. Ma, J.F. Liu, X.M. Sun, D.Y. Zhao, D.G. Evans, J. Am. Chem. Soc. 132 (2010) 2333.
[19] S. Ghosh, S.M. Bachilo, R.B. Weisman, Nat. Nano 5 (2010) 443.
[20] J.P. Novak, C. Nickerson, S. Franzen, D.L. Feldheim, Anal. Chem. 73 (2001) 5758.
[21] A. Akthakul, A.I. Hochbaum, F. Stellacci, A.M. Mayes, Adv. Mater. 17 (2005) 532.
[22] T.H. Ha, Y.J. Kim, S.H. Park, Chem. Commun. 46 (2010) 3164.
[23] K. Park, H. Koerner, R.A. Vaia, Nano Lett. 10 (2010) 1433.
[24] B.P. Khanal, E.R. Zubarev, J. Am. Chem. Soc. 130 (2008) 12634.
[25] W. Ni, X. Kou, Z. Yang, J.F. Wang, ACS Nano 2 (2008) 677.
[26] X.Y. Xu, K.K. Caswell, E. Tucker, S. Kabisatpathy, K.L. Brodhacker, W.A. Scrivens, J. Chromatogr. A 1167 (2007) 35.
[27] V. Sharma, K. Park, M. Srinivasarao, Proc Natl. Acad. Sci. U.S.A. 106 (2009) 4981.
[28] X. Huang, I.H. El-Sayed, W. Qian, M.A. El-Sayed, J. Am. Chem. Soc. 128 (2006) 2115.
[29] C. Yu, H. Nakshatri, J. Irudayaraj, Nano Lett. 7 (2007) 2300.
[30] Y.F. Huang, H.T. Chang, W. Tan, Anal. Chem. 80 (2008) 567.
[31] A.K. Salem, P.C. Searson, K.W. Leong, Nat. Mater. 2 (2003) 668.
[32] C.C. Chen, Y.P. Lin, C.W. Wang, H.C. Tzeng, C.H. Wu, Y.C. Chen, C.P. Chen, L.C. Chen, Y.C. Wu, J. Am. Chem. Soc. 128 (2006) 3709.
[33] Q. Wei, J. Ji, J. Shen, Macromol. Rapid Commun. 29 (2008) 645.
[34] S.M. Marinakos, S. Chen, A. Chilkoti, Anal. Chem. 79 (2007) 5278.
[35] A.K. Oyelere, P.C. Chen, X. Huang, I.H. El-Sayed, M.A. El-Sayed, Bioconjug. Chem. 18 (2007) 1490.
[36] G.J. Nusz, A.C. Curry, S.M. Marinakos, A. Wax, A. Chilkoti, ACS Nano 3 (2009) 795.
[37] K. Imura, T. Nagahara, H. Okamoto, J. Phys. Chem. B 109 (2005) 13214.
[38] H.F. Wang, T.B. Huff, D.A. Zweifel, W. He, P.S. Low, A. Wei, J.X. Cheng, Proc Natl. Acad. Sci. U.S.A. 102 (2005) 15752.
[39] C. Sönnichsen, A.P. Alivisatos, Nano Lett. 5 (2005) 301.
[40] L.H. Xiao, Y.X. Qiao, Y. He, E.S. Yeung, Anal. Chem. 82 (2010) 5268.
[41] B. Nikoobakht, M.A. El-Sayed, Chem. Mater. 15 (2003) 1957.
[42] X. Sun, D. Luo, J. Liu, D.G. Evans, ACS Nano 4 (2010) 3381.
[43] G.K. Youngren, A. Acrivos, J. Fluid Mech. 69 (1975) 377.
[44] K. Zhou, J.Z. Lin, Fibers Polym. 9 (2008) 39.
[45] O. Bernstein, M. Shapiro, J. Aerosol Sci. 25 (1994) 113.
[46] G. Kasper, T. Niida, M. Yang, J. Aerosol Sci. 16 (1985) 535.
[47] G. Kasper, Aerosol Sci. Technol. 1 (1982) 187.
[48] Z. Dogic, A.P. Philipse, S. Fraden, J.K.G. Dhont, J. Chem. Phys. 113 (2000) 8368.